Time resolution studies using digital constant fraction discrimination

A. Fallu-Labruyere*, H. Tan, W. Hennig, W.K. Warburton

XIA LLC, 31057 Genstar Road, Hayward, CA 94544, USA

Available online 6 April 2007

Abstract

Digital Pulse Processing (DPP) modules are being increasingly considered to replace modular analog electronics in medium-scale nuclear physics experiments (100–1000s of channels). One major area remains, however, where it has not been convincingly demonstrated that DPP modules are competitive with their analog predecessors—time-of-arrival measurement. While analog discriminators and time-to-amplitude converters can readily achieve coincidence time resolutions in the 300–500 ps range with suitably fast scintillators and Photomultiplier Tubes (PMTs), this capability has not been widely demonstrated with DPPs. Some concern has been expressed, in fact, that such time resolutions are attainable with the 10 ns sampling times that are presently commonly available.

In this work, we present time-coincidence measurements taken using a commercially available DPP (the Pixie-4 from XIA LLC) directly coupled to pairs of fast PMTs mated with either LSO or LaBr$_3$ scintillator crystals and excited by ^{22}Na γ-ray emissions. Our results, 886 ps for LSO and 576 ps for LaBr$_3$, while not matching the best literature results using analog electronics, are already well below 1 ns and fully adequate for a wide variety of experiments. These results are shown not to be limited by the DPPs themselves, which achieved 57 ps time resolution using a pulser, but are degraded in part both by the somewhat limited number of photoelectrons we collected and by a sub-optimum choice of PMT. Analysis further suggests that increasing the sampling speed would further improve performance. We therefore conclude that DPP time-of-arrival resolution is already adequate to supplant analog processing in many applications and that further improvements could be achieved with only modest efforts.

© 2007 Elsevier B.V. All rights reserved.

PACS: 78.47; 39.90; 84.30.S; 29.40.M; 06.30.F; 07.75; 82.80.R

Keywords: Digital spectrometer; TOF; CFD; Fast scintillators

1. Introduction

Intermediate scale nuclear experiments requiring 100–1000's of electronic signal processing channels are not well served at present either by conventional modular (e.g. NIM) electronics or by ASICs. The former are bulky, expensive and difficult to set up, calibrate and re-configure by hand on a large scale, while the latter have long expensive development cycles, cannot be reconfigured to adapt to changing needs, and typically sacrifice some performance to meet compactness and low-power requirements. Digital Pulse Processing (DPP) modules with relatively high densities at a reasonable cost per channel have become available that implement many of the classical analog processing functions (i.e. pulse discrimination, energy filtering, pile-up inspection, and coincidence and multiplicity triggering) at least as well as modular analog electronics. Further, these DPP modules are more readily scalable to larger experiments than simple trace digitizers because their on-board processing can substantially reduce the amount of bandwidth needed to export event data over data buses.

Thus, since DPP technology appears to be otherwise scalable to these intermediate experiments, we decided to benchmark its Time-of-Flight (TOF) capability to determine whether that too could match or surpass the analog state of the art. We therefore undertook to develop a Constant Fraction Discriminator (CFD) that could be readily implemented in a Field Programmable Gate Array (FPGA) and tested it with both a digital pulser and in coincidence timing measurements using fast scintillators

---

*Corresponding author.

E-mail address: anthony@xia.com (A. Fallu-Labruyere).

and PMTs. Obtaining results that are competitive but not state of the art, we also investigated the factors limiting our results in order to set the stage for future improvements.

2. Material and methods

2.1. DGF-Pixie Hardware

For a DPP module we used the DGF Pixie-4 and Pixie-16, members of XIA LLC's DGF-Pixie family. These multi-channel coincidence spectrometers with a Compact PCI interface share clock and trigger signals over a PXI backplane and are intended for small to medium nuclear physics setups [1]. The 4-channel Pixie-4 (3U format) is flexible enough for small prototype systems, and the 16-channel Pixie-16 (6U format) handles larger channel count applications. After DC coupled amplification and Nyquist filtering, the modules directly digitize their input signals and implement pulse detection, energy filtering, pile-up inspection and discrimination operations all digitally, primarily in an FPGA, with a Digital Signal Processor (DSP) available for more complex operations. They have onboard memory for storing spectra and captured traces and can export data over the PXI bus at up to 100 MB/s.

2.2. CFD development

$$\int \mathrm{CFTrace}[k] = \sum_{i=1}^{L} \{F * \mathrm{Trace}[k-i] - \mathrm{Trace}[k-i-D]\}. \tag{1}$$

Our first task was to develop an algorithm that would be "FPGA friendly" so that, if successful, it could easily be implemented. We therefore investigated processes of the form shown in Eq. (1), which digitally approximates the classic analog CFD by subtracting a pulse's signal trace delayed by D from a fraction F of the original trace and then computing the resultant signal's first zero crossing to digitally estimate the pulse's time-of-arrival. The running averaging of length L is for noise reduction. This class of CFD is readily implemented in modern FPGAs using FIFOs (for D), shift registers (for F), and accumulators (for L). Linear interpolation can either be done in the FPGA through successive approximations or carried out in the DSP [1]. In this work, we computed zero crossing times by simple linear interpolation between the first CFTrace points above and below zero. To optimize the filter, we captured signals in several timing situations described below, processed them offline using Eq. (1), and adjusted D, F and L to obtain the best timing resolution.

Fig. 1 shows a typical LSO scintillator trace, together with CFTrace computed using values $L = D = 1$ and $F = 0.5$. As shown, these pulses have sufficiently fast risetimes that the zero crossing point lies well up on the pulse's rising edge and thus may show a certain amount of jitter, depending upon the arrival time of the pulse relative
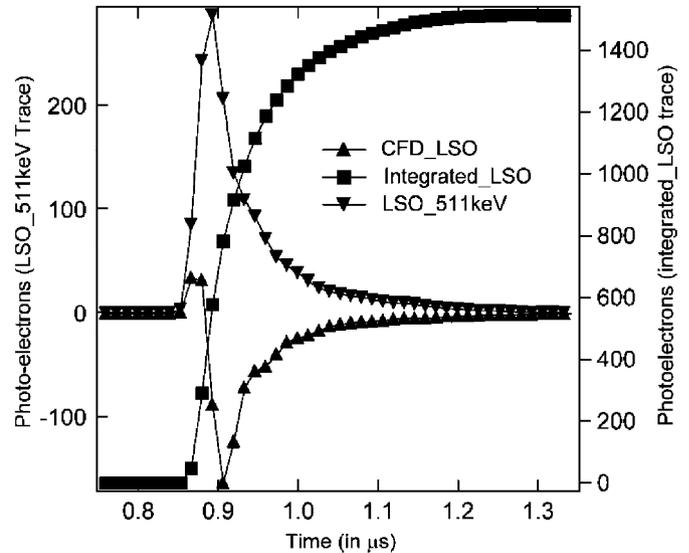
Fig. 1. PMT output pulse and computed CFTrace ($L = D = 1$, $F = 0.5$) from a 511 keV event in LSO. The integral of the PMT pulse is also shown.

to the digital clock's edge transitions. The maximum of the shown pulse integral is proportional to the number of photoelectrons collected, a point that we will discuss later.

2.3. TOF setups

We generated TOF signals in two ways. The first was using an in-house pulser that makes up to 16-buffered copies of arbitrary waveforms generated digitally in an FPGA and fed to a fast 14-bit Digital–to-Analog Converter (DAC). With the pulser set to produce pulses having 50 ns risetimes and 2.5 μs exponential decay times, its outputs were connected to pairs of DGF-Pixie inputs using RG-58 cables of calibrated lengths (equal or unequal) to create pulses having precisely separated arrival times.

The second signal source was from a pair of fast Photonis XP2020 2" PMTs, both coupled either to $2 \times 2 \times 3 \, \mathrm{mm}^3$ LSO crystals (unwrapped) or to 1 in. diameter by 1 in. high LaBr$_3$ crystals (Teflon wrapped and canned), and facing oppositely a 1 μCi ^{22}Na source. The PMTs were biased at -1700 and -1350 V for LSO and LaBr$_3$ respectively for photocurrent non-linearity below 1%. Typical count rates were 100 cps for LSO and 4,000 cps for LaBr$_3$. Fig. 2 shows energy resolutions obtained from the LSO (12%), LaBr$_3$ (3.9%) and the pulser (0.04%). We note degraded energy resolution from the tiny unwrapped LSO crystals.

2.4. Trace capture

The Pixie-4 and Pixie-16 were configured to capture data only for detected coincidence events. Thus, when either channel's fast trigger filter detected a pulse it issued a fast wired-OR trigger and started its FIFO collecting a digitized signal trace. When the pulse was validated after pile-up
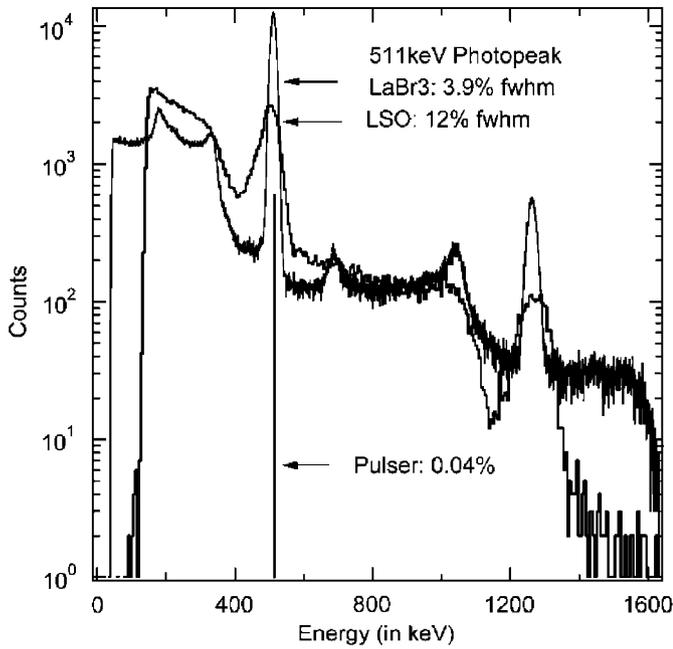
Fig. 2. Energy spectra from LSO, LaBr$_3$, and digital pulser.

Fig. 3. TOF spectra from the pulser and from LSO and LaBr$_3$ at 511 keV. $F = 0.4$–0.7, $D = 1$, and $L = 1$ in all cases.

inspection, all FIFOs were stopped on the next clock edge transition. The DSP polled both channels to look for coincidences, and if both channel triggered, read out the FIFOs. The phase of captured signal traces is thus fixed with a stability limited only by the ADC sampling clock edge jitter which, as we shall see, is very small. The sampling period was 13.33 ns.

3. Results

Fig. 3 shows our results: TOF spectra from the three-signal sources using delay cables of equal lengths. The small LSO crystals gave the worst time resolution: 886 ps FWHM, while we were able to achieve 576 ps with the faster LaBr$_3$ crystals. We attribute the asymmetry in the LSO time spectrum to difficulties in attaching the very small LSO crystals reliably to the face of the PMT. Using the pulser, we measured time resolutions between 57 and 100 ps (see Section 4.2). Fig. 3 shows an average value of 80 ps.

4. Discussions

4.1. Comparison to reported analog results

The best analog results that we found in the literature for LSO and LaBr$_3$ are significantly better than those reported here. Thus, in a careful study of time resolution versus number of collected photoelectrons, Aykac's [2] best result using LSO at 511 keV was 425 ps time resolution, which is 52% better than our result. Working with LaBr$_3$, Karp [3] reported coincidence timing resolution of 313 ps, or 45% better than our result. The obvious question, then, is "What is the source of these differences?"

Fig. 4. Time resolution versus time of flight. The insert shows the reconstructed energy spectrum from the pulser.

4.2. Hardware "intrinsic" time resolution

The first obvious suspect was the digital spectrometer itself. We studied this possibility as follows. Starting with two Pixie-4 channels that shared a common FPGA and using our digital pulser, we measured TOF resolution versus cable delay, as shown in Fig. 4, where we varied TOF from zero to 128 ns.

As shown, within experimental error, time resolution increased essentially linearly with cable delay, ranging from 57 ps for zero delay to 86 ps for the full 128 ns delay. The primary source of this loss of time resolution was attenuation in the cables, which would effectively reduce signal-to-noise in our CFTrace signal, which is essentially a derivative of the input signal. Repeating the measurements using two Pixie-4 channels that shared different FPGAs on the same Pixie-4 card, we measured a minimum TOF resolution of 68 ps for zero cable delay. Repeating again using the same channel in two neighboring Pixie-4 cards on the same PXI backplane, we measured a TOF resolution of 117 ps. Finally, using Pixie-16 modules (which have more complex internal digital logic circuitry) we repeated this measurement between two cards in a single 6U PXI crate, measuring 150 ps TOF resolution. As expected, the Pixie-16 modules have slightly worse time resolution than the Pixie-4's, due to their more complex circuitry, but in no case, when added in quadrature, would any of these values cause more than a small fraction of the resolution differences between our results and the best analog results. Further, these results also show that the need for multiple modules will not affect the DGF Pixie DPP technology's ability to be scaled to larger systems.

We therefore determine that the Pixie-4's TOF capability is not inherently limited by the time stability of its digital logic or jitter in its clocks. Rather, since the pulser signal actually had a slower risetime than the scintillator signals, we suspect that the accuracy of our zero crossing method is limited by the limited number of points on the scintillator pulses' rising edges. If true, then improvements in TOF resolution could be obtained either by increasing the sampling speed, slowing down the signals somewhat by reducing their bandwidth, or by devising a CFD algorithm that requires fewer leading edge points.

4.3. Number of photons

Since it is also known that time resolution depends upon the number of photoelectrons collected, we also measured our absolute gain so that we could compare our results to those of Aykac [2] at equal numbers of photoelectrons. Since we could not observe a single photoelectron peak at the low gain required to operate with 511 keV photons, we therefore made measurements at increased voltages and extrapolated the gain to our actual operating voltage.

Fig. 5 shows the results of these measurements and the extrapolation. Measurements were made at −1900 V, −2000 V, and −2100 V and the resultant single photoelectron peaks (as shown in the inset in Fig. 5) were fitted to determine the MCA channel as a function of PMT operating voltage. The fit to these three values was then extrapolated to the actual PMT operating voltage of −1700 V. Knowing the MCA channel for a single photoelectron then allowed us to determine that at 511 keV we were collecting 1480 photoelectrons. At this value, Aykac [2] reported a time resolution of 600 ps, which is still over 30% better
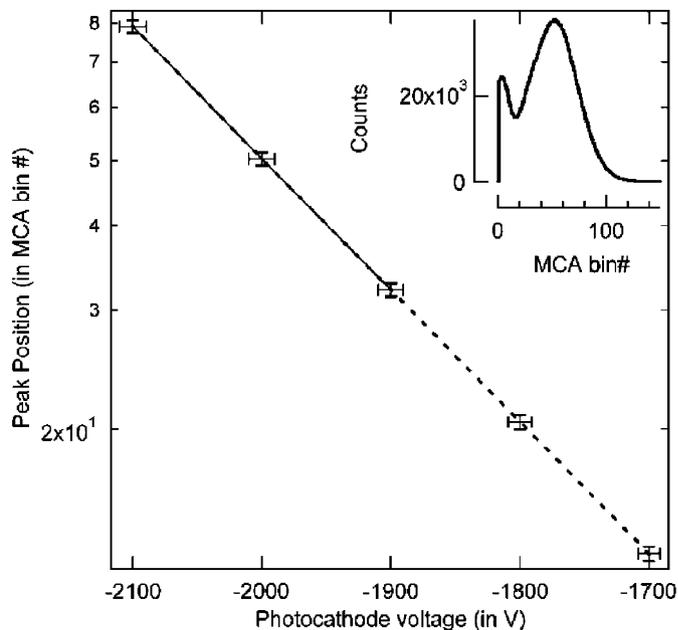
Fig. 5. Determination of single photoelectron peak position. The inset shows a spectrum taken at −2000 V. The peak to valley ratio is $2.52 \pm 1\%$ and the peak FWHM is 87%.

than our value of 886 ps. Thus, while light collection efficiency was clearly one factor, the issues identified in Section 4.2 are still clearly more significant.

Another issue was choice of PMT. While the XP2020, with its 12 dynodes is appropriate for LSO, a better choice for the brighter scintillator $LaBr_3$ would have been the XP20D0, as used by Karp [3]. This tube, with only eight dynodes, has less transit time jitter and better quantum efficiency [4]. Finally, the smaller crystal geometries ($4 \times 4 \times 30 \, mm^3$) used by Karp [3] lead to more focused photoelectrons, which reduces their transit time spread somewhat, compared to the chosen geometry.

5. Conclusions

Using LSO, $LaBr_3$, and a pulser, we studied the timing performance of a CFD algorithm that could be easily implemented in a modern FPGA. When optimized, this algorithm obtained time resolutions of 886 ps for LSO and 576 ps for $LaBr_3$, which is adequate for a wide variety of timing work. This implies that the DGF-Pixie DPP technology can therefore be successfully scaled to large channel count nuclear data collection applications.

Our achieved coincident time resolutions, however, were still significantly poorer than the best values reported using analog technology, especially in the case of the faster scintillator $LaBr_3$. Our analysis suggests that this results from the short signal risetime relative to the 13.33 ns sampling period and that improvements could be obtained by reducing sampling times, the risetimes, or devising a less risetime sensitive algorithm.

Acknowledgments

References

[1] W. Hennig, et al., The DGF Pixie-4 spectrometer—compact digital readout electronics for HPGe clover detectors, presented at the IRRMA Fifth Conference, June 2005, Hamilton, ON, Canada, NIM B, in press.

[2] M. Aykac, et al., Timing performance of Hi-Rez detector for time-of-flight (TOF) PET, in: IEEE–NSS 2005 Conference Record M07–131.

[3] J.S. Karp, et al., Characterization of a time-of-flight PET scanner based on Lanthanum Bromide, in: IEEE–NSS 2005 Conference. Record M04–8.

[4] F. Bauer, et al., Performance study of the new Hamamatsu R9779 & Photonis XP20D0 fast 2'' Photomultipliers, in: IEEE–NSS 2005 Conference Record J03–08.